

HUTFormer: Hierarchical U-Net Transformer for Long-Term Traffic Forecasting

ZeZhi Shao, Fei Wang, Zhao Zhang, Yuchen Fang, Guangyin Jin, Yongjun Xu

Abstract—Traffic forecasting, which aims to predict traffic conditions based on historical observations, has been an enduring research topic and is widely recognized as an essential component of intelligent transportation. Recent proposals on Spatial-Temporal Graph Neural Networks (STGNNs) have made significant progress by combining sequential models with graph convolution networks. However, due to high complexity issues, STGNNs only focus on short-term traffic forecasting, *e.g.*, 1-hour forecasting, while ignoring more practical long-term forecasting. In this paper, we make the first attempt to explore long-term traffic forecasting, *e.g.*, 1-day forecasting. To this end, we first reveal its unique challenges in exploiting multi-scale representations. Then, we propose a novel *Hierarchical U-net Transformer* (HUTFormer) to address the issues of long-term traffic forecasting. HUTFormer consists of a hierarchical encoder and decoder to jointly *generate* and *utilize* multi-scale representations of traffic data. Specifically, for the encoder, we propose window self-attention and segment merging to extract multi-scale representations from long-term traffic data. For the decoder, we design a cross-scale attention mechanism to effectively incorporate multi-scale representations. In addition, HUTFormer employs an efficient input embedding strategy to address the complexity issues. Extensive experiments on four traffic datasets show that the proposed HUTFormer significantly outperforms state-of-the-art traffic forecasting and long time series forecasting baselines.

Index Terms—Traffic forecasting, long-term time series forecasting, multivariate time series forecasting.



1 INTRODUCTION

Traffic forecasting aims at predicting future traffic conditions (*e.g.*, traffic speed or flow) based on historical traffic conditions observed by sensors. With the development of Intelligent Transportation Systems (ITS), traffic forecasting fuels a wide range of services related to traffic scheduling, public safety, *etc.* [1], [2]. For example, predicting long-term traffic changes (*e.g.*, 1 day) is valuable for people to plan their route in advance to avoid possible traffic congestion.

In general, traffic data consists of multiple time series, where each time series records traffic conditions observed by sensors deployed on a road network. A critical property of traffic data is that there exist strong correlations between time series owing to the connection of road networks [3]. To make accurate traffic forecasting, state-of-the-art proposals [1], [3], [4], [5] usually adopt Spatial-Temporal Graph Neural Networks (STGNNs), which model the correlations between time series based on Graph Convolution Networks (GCNs) [3], [6], [7]. However, there is no free lunch. Graph convolution brings significant improvements in performance and complexity at the same time. Computational complexity usually increases linearly or quadratically with the length and number of time series [8]. Therefore, it is difficult for STGNNs to scale to long-term historical traffic data, let alone predict long-term future traffic conditions. In fact, most existing works focus on short-term traffic prediction,

ZeZhi Shao, Fei Wang, Zhao Zhang, and Yongjun Xu are with the Institute of Computing Technology, CAS, Beijing 100190, China. ZeZhi Shao is also with the University of Chinese Academy of Sciences, Beijing 100049, China. (e-mail: {shaozeZhi19b, wangfei, zhangzhao2021, xjy}@ict.ac.cn)
Yuchen Fang is with the University of Electronic Science and Technology of China (e-mail: fyclmiss@gmail.com)
Guangyin Jin is with the National University of Defense Technology (e-mail: jinguangyin96@foxmail.com)
Corresponding Author: Fei Wang, wangfei@ict.ac.cn.

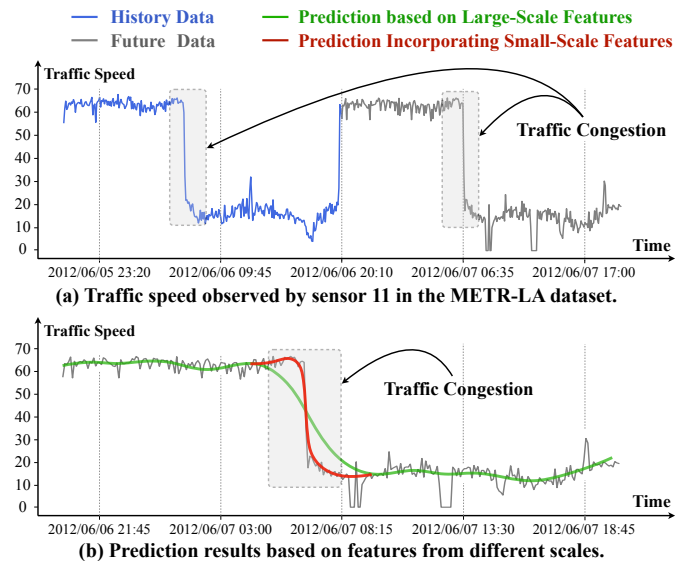


Fig. 1. Examples of long-term traffic forecasting. Note that the figure below is the future part of the picture above.

e.g., predicting future 12 time steps (1 hour in commonly used datasets). Such an inability to make long-term traffic forecasting limits the practicality of these models.

In this paper, we focus on long-term traffic forecasting, *e.g.*, predicting a future day. Except for the correlations between time series, we argue that the long-term traffic forecasting task has its own uniqueness. In the following, we discuss them in detail to motivate model design. An example of traffic data is shown in Figure 1(a). On the one hand, when observing from a global perspective, traffic data usually exhibit regular changes, *e.g.*, daily periodicity. On

the other hand, local details are also extremely important for traffic forecasting. For example, we must capture the rapidly decreasing traffic changes when daily traffic congestion occurs. To capture these different patterns, we argue that exploiting multi-scale representations of traffic data is the key challenge of accurate long-term traffic forecasting. Specifically, smaller-scale and larger-scale representations are extracted based on smaller and larger receptive fields, respectively. The former is usually semantically weak but fine-grained, which facilitates the prediction of local details, *e.g.*, rapid changes during traffic congestion. In contrast, the latter is coarse-grained but semantically strong, which is helpful in predicting global changes, *e.g.*, daily periodicity. An illustration is shown in Figure 1(b). The prediction based on large-scale features captures daily periodicity but misses local details, which can be fixed by further incorporating small-scale features.

However, it is a challenging task to exploit multi-scale representations of traffic data. We discuss it from two aspects: *generating* and *utilizing* multi-scale representations. *On the one hand*, most existing models cannot generate multi-scale representations of traffic data. State-of-the-art models for long-sequence time series forecasting [9] mainly adopt Transformer architecture to capture the long-term dependencies based on self-attention mechanisms [10]. However, standard self-attention naturally has a global receptive field and thus can only generate representations on a fixed scale. *On the other hand*, utilizing multi-scale representations for traffic forecasting is also a challenging task, as it usually requires a specific decoder. For example, in computer vision tasks like object detection and semantic segmentation, researchers designed decoders such as FPN [11] and U-Net [12] to utilize the multi-scale representations extracted by the pre-trained CNN [13] encoder. These architectures usually require pixel alignment of input and output images. However, the historical and future sequences in traffic forecasting problems are not the same sequences, *i.e.*, not aligned, making existing approaches [11], [12] inapplicable.

Based on the above discussion, we summarize three challenges that the desired long-term traffic forecasting model should address. First, it must *efficiently* model the correlations between multiple long-term time series. Second, it should *generate* multi-scale representations of traffic data by an encoder. Third, it should include a decoder for traffic forecasting tasks to effectively *utilize* the multi-scale representations generated by the encoder.

To address the above challenges, we propose a novel *Hierarchical U-net TransFormer* (named HUTFormer). As shown in Figure 2, HUTFormer is a two-stage model consisting of a hierarchical encoder and a hierarchical decoder, forming an inverted U-shaped structure. *To address the efficiency problem*, HUTFormer designs an efficient input embedding strategy, which employs segment embedding and spatial-temporal positional encoding to significantly reduce the complexity of modeling multiple long-term time series in both temporal and spatial dimensions. *To generate multi-scale representations*, the HUTFormer encoder proposes a window Transformer layer to limit the receptive field, and then designs segment merging as a pooling layer to extract larger-scale features. Thus, lower layers of the encoder focus on smaller-scale features, while higher layers generate larger-scale features.

Then, HUTFormer makes an intermediate prediction based on the top-level representations. *To utilize multi-scale representations*, the HUTFormer decoder proposes a cross-scale attention mechanism to address the misalignment issue, which retrieves information for each segment of the intermediate prediction from multi-scale representations, thus enabling the fine-tuning of the intermediate prediction. By exploiting the multi-scale representations of traffic data, HUTFormer is capable of making accurate long-term traffic forecasting. The main contributions of this paper are summarized as follows:

- To our best knowledge, this is the first attempt to study long-term traffic forecasting. We reveal its unique challenges in exploiting multi-scale representations of traffic data, and propose a novel *Hierarchical U-net TransFormer* (HUTFormer) to address them.
- We propose window self-attention and cross-scale attention mechanisms to generate and utilize multi-scale representations effectively. In addition, to address complexity issues, we design an input embedding strategy that includes segment embedding and spatial-temporal positional encoding.
- Extensive experiments on four traffic datasets show that the proposed HUTFormer significantly outperforms state-of-the-art traffic forecasting and long-sequence time series forecasting baselines, and effectively exploits the multi-scale representations of traffic data.

2 RELATED WORK

2.1 Traffic Forecasting

Previous traffic forecasting studies usually fall into two categories, *i.e.*, knowledge-driven (*e.g.*, queuing theory [14]) and early data-driven (*e.g.*, sequential models [15], [16], [17], [18]). However, these methods usually ignore the correlation between time series and the high non-linearity of time series [1], which severely limits the effectiveness of these methods. To this end, Spatial-Temporal Graph Neural Networks (STGNNs) were proposed recently [3] to model the complex spatial-temporal correlations in traffic data. Specifically, STGNNs combine Graph Neural Networks (GNNs) [6], [7] and sequential models (*e.g.*, CNN [18] or RNN [16]), to model the complex spatial-temporal correlation in traffic data. For example, DCRNN [3], ST-MetaNet [19], AGCRN [20], *etc.* [21], [22], [23], are RNN-based methods, which combine GNN with recurrent neural networks. Graph WaveNet [4], MTGNN [24], STGCN [22], and StemGNN [25] are CNN-based methods [26], which usually combines GNN with the Temporal Convolution Network (TCN [18]). Moreover, the attention mechanism is also a widely used technique in STGNNs [27], [28], [29], [30], [31]. Although STGNNs have achieved significant progress, their complexity is high. Specifically, their complexity usually increases linearly or quadratically with the length and the number of time series [8], since they need to deal with both temporal and spatial dependency at every step. Thus, most of them focus on short-term traffic forecasting based on short-term history data, *e.g.*, predicting future 1-hour traffic conditions based on 1-hour historical data. A recent work STEP [8] attempts to address this issue based on the time series pre-training model. It significantly enhances STGNN's

ability to exploit long-term historical data. However, STEP requires a downstream STGNN as the backbone, which still focuses on short-term traffic forecasting.

Although STGNN-based traffic forecasting has made significant progress, these models only focus on short-term traffic forecasting, and cannot handle long-term traffic forecasting. On the one hand, due to the high complexity, most of them can not handle long-term history data, let alone predict long-term future traffic conditions. On the other hand, apart from efficiency issues, long-term traffic forecasting also has its unique challenges, which require exploiting multi-scale representations of traffic data to capture the complex long-term traffic dynamics.

2.2 Long-Sequence Time Series Forecasting

Recently, long-sequence time series forecasting [9] has received much attention [9], [32], [33], [34], [35], [36], [37]. They aim to make long-term future predictions by modeling long-term historical sequences. For example, Informer [9] proposes a ProbSparse self-attention mechanism to replace the standard self-attention, which enhances the predictive ability of the standard Transformer in the long-sequence forecasting problem. Autoformer [32] designs an efficient Auto-Correlation mechanism to conduct dependencies discovery and information aggregation at the series level. DLinear [35] rethinks Transformer-based techniques and proposes a simple linear model based on decomposition to achieve better accuracy.

Although these models have made considerable progress in long-term time series forecasting, they are not designed for traffic data, which significantly affects their effectiveness in traffic forecasting problems. We discuss it from two aspects. First of all, there are strong correlations between multiple time series in traffic data, which is an important bottleneck in traffic forecasting [3]. However, long-sequence time series forecasting models usually do not pay attention to such spatial correlations. Second, as discussed in Section 1, long-term traffic forecasting requires exploiting multi-scale representations of traffic data to capture the complex long-term traffic dynamics. However, long-sequence forecasting models usually rely on the self-attention mechanism and its variants, which can not explicitly generate multi-scale features.

3 PRELIMINARIES

4 NOTATION TABLE

In this section, we define the notions of traffic data and traffic forecasting task. Frequently used notations are summarized in Table 1.

Definition 1. Traffic Data $\mathcal{X} \in \mathbb{R}^{T \times N \times C}$ denotes the observation from all sensors on the traffic network, where T is the number of time steps, N is the number of traffic sensors, and C is the number of features collected by sensors. We additionally denote the data from the sensor i as $\mathbf{X}^i \in \mathbb{R}^{T \times C}$.

Definition 2. Traffic Forecasting aims to predict the traffic values $\mathcal{Y} \in \mathbb{R}^{T_f \times N \times C}$ of the T_f nearest future time steps based on the given historical traffic data $\mathcal{X} \in \mathbb{R}^{T_h \times N \times C}$

TABLE 1
Frequently used notation.

Notations	Definitions
T	The length of history traffic data.
T_f	The length of future traffic data.
N	The number of time series.
C	The number of feature channels in a traffic sensor.
\mathcal{X}	History data of shape $\mathbb{R}^{T \times N \times C}$
\mathcal{Y}	Future data of shape $\mathbb{R}^{T_f \times N \times C}$
\mathbf{X}^i	History data of sensor i .
\mathbf{Y}^i	Future data of sensor i .
$\hat{\mathbf{Y}}^i$	Prediction data of sensor i .
L	The segment size.
P	The number of segments. $T = P \times L$.
d	The hidden dimension.
\mathbf{W}	Parameter matrix of the fully connected layer.
\mathbf{b}	Parameter of the bias of the fully connected layer.
\mathbf{E}	Spatial embeddings of shape $\mathbb{R}^{N \times d_1}$.
\mathbf{T}	Temporal embeddings.
N_D	The number of time slots of a day.
N_W	The number of days in a week (7).
\mathbf{S}	Embeddings of each segment after segment embedding.
\mathbf{U}	Embeddings of each segment after spatial-temporal positional encoding.
\mathbf{H}	Hidden states.

from the past T_h time steps. In this paper, we focus on long-term traffic forecasting, e.g., forecasting for a day in the future.

5 MODEL ARCHITECTURE

5.1 Overview

As illustrated in Figure 2, HUTFormer is based on a hierarchical U-net structure to *generate* and *utilize* multi-scale representations of traffic data. In this subsection, we intuitively discuss each component of HUTFormer and its two-stage training strategy.

First, we discuss the hierarchical encoder. The window Transformer layer is the basis for generating multi-scale representations, which calculates self-attention within a small window to limit the receptive field. Then, segment merging acts as a pooling layer, reducing the sequence length to produce larger-scale representations. By combining them, lower layers can focus on smaller-scale features while higher layers focus on larger-scale features, thus successfully generating multi-scale features. Then, an intermediate prediction is made based on the top-layer representations. However, considering that the top-layer features are semantically strong but coarse-grained, the intermediate prediction may fail to capture rapidly changing local details, e.g., the red line in Figure 1(b).

To address the above problem, the hierarchical decoder aims to fine-tune the intermediate prediction by incorporating multi-scale representations. U-net [12], [38] is a popular structure for utilizing multi-scale representations, especially in computer vision tasks (e.g., semantic segmentation). In these tasks, the pixels of the input and target images are aligned, i.e., models operate on the same image. However, for traffic forecasting tasks, the input and output sequences are not the same sequence, i.e., not aligned. Thus, the representations generated by the encoder and the decoder cannot

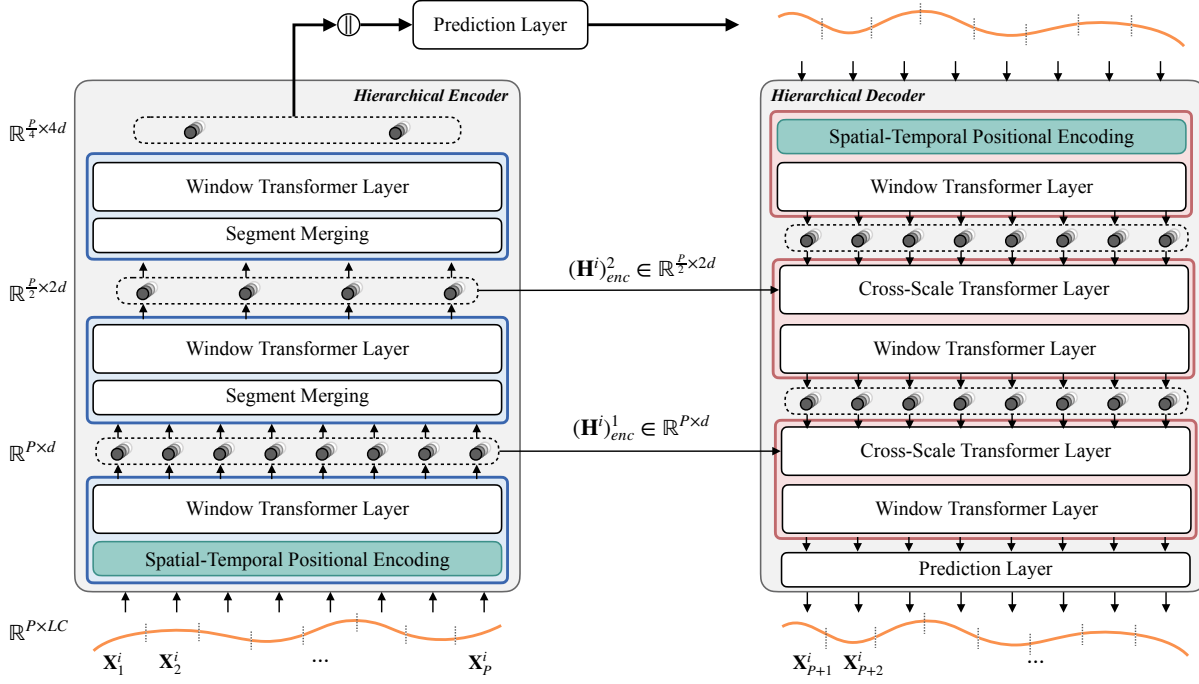


Fig. 2. The overview of the proposed HUTFormer. *Left*: the hierarchical encoder. It generates multi-scale features for traffic data based on window Transformer layer and segment merging, and makes an intermediate prediction. *Right*: the hierarchical decoder. It fine-tunes the intermediate prediction by incorporating multi-scale features based on cross-scale Transformer layer. In addition, segment embedding and spatial-temporal positional encoding are proposed to address complexity issues.

be directly superimposed as regular U-net structures [12], [38] do for computer vision tasks. To this end, we design a cross-scale Transformer layer, which uses the representations from the decoder as *queries* and the multi-scale features from the encoder as *keys* and *values* to retrieve information. Such a top-down pathway and lateral connects help to combine the multi-scale representations, thus enhancing the prediction accuracy.

In addition, HUTFormer addresses complexity issues based on an efficient input embedding strategy, which consists of segment embedding and spatial-temporal positional encoding. On the one hand, segment embedding reduces complexity from the temporal dimension by using time series segments as basic input tokens. This simple operation has significant benefits in both reducing the length of the input sequence and providing more robust semantics [8]. On the other hand, spatial-temporal positional encoding is designed to replace the standard positional encoding [10], [39] in Transformer. More importantly, it efficiently models the correlations among time series from the perspective of solving the indistinguishability of samples [40], [41], avoiding the high complexity of conducting graph convolution [3], [4] in the spatial dimension.

Finally, we propose the training strategy: a two-stage strategy. The first stage aims to train the hierarchical encoder based on the Mean Absolute Error (MAE) between the intermediate prediction and ground truth. In the second stage, we only train the decoder, while the parameters of the encoder are fixed to act as the multi-scale feature extractor. The reason for adopting the two-stage strategy is that traffic forecasting tasks are different from tasks that employ an end-to-end strategy (*e.g.*, semantic segmentation [12], [38]

and object detection [11] in computer vision). Specifically, in computer vision tasks, pre-trained vision models (*e.g.*, pre-trained ResNet [13]) usually serve as the backbone to extract multi-scale features [11]. However, there is no pre-trained model for time series that can extract multi-scale features. Therefore, optimizing the feature extractor (*i.e.*, the encoder) and downstream networks (*i.e.*, the decoder) in an end-to-end fashion may be insufficient. The experimental results in Section 6.5 also verify this hypothesis. Next, we introduce each component in detail.

5.2 Input Embedding

Segment embedding. Most previous works usually use single data points as the basic input units. However, isolated points of time series usually give less semantics [8] and are more easily affected by noise. Therefore, HUTFormer adopts segment embedding, *i.e.*, dividing the input sequence into several segments to get the input tokens. Specifically, given the time series $\mathbf{X}^i \in \mathbb{R}^{T \times C}$ from sensor i , HUTFormer divides it into P non-overlapping segments of length L , *i.e.*, $T = P * L$. We denote the j th segment as $\mathbf{X}_j^i \in \mathbb{R}^{LC}$. Then, we conduct the input embedding layer based on these segments:

$$\mathbf{S}_j^i = \mathbf{W} \cdot \mathbf{X}_j^i + \mathbf{b}, \quad (1)$$

where $\mathbf{S}_j^i \in \mathbb{R}^d$ is the embedding of segments j of the time series from sensor i , and d is the hidden dimension. $\mathbf{W} \in \mathbb{R}^{d \times (LC)}$ and $\mathbf{b} \in \mathbb{R}^d$ are learnable parameters shared by all segments.

In summary, applying segment embedding brings two benefits. First, it provides more robust semantics. Second, it significantly reduces the sequence length to reduce computational complexity.

Spatial-temporal positional encoding. In this paper, we propose to replace the standard positional encoding in Transformer-based networks [10], [39] with Spatial-Temporal Positional Encoding (ST-PE). Specifically, given the segment embedding $\mathbf{S}_j^i \in \mathbb{R}^d$ of segments j from time series i , ST-PE conduct positional encoding on the spatial and temporal dimensions simultaneously:

$$\mathbf{U}_j^i = \text{Linear}(\mathbf{S}_j^i \parallel \mathbf{E}^i \parallel \mathbf{T}_j^{TiD} \parallel \mathbf{T}_j^{DiW}). \quad (2)$$

On the spatial dimension, we define the spatial positional embeddings $\mathbf{E} \in \mathbb{R}^{N \times d_1}$, where N is the number of time series (*i.e.*, sensors), and d_1 is the hidden dimension. On the temporal dimension, we define two semantic positional embeddings, $\mathbf{T}^{TiD} \in \mathbb{R}^{N_D \times d_2}$ and $\mathbf{T}^{DiW} \in \mathbb{R}^{N_W \times d_3}$, where N_D is the number of time slots of a day (determined by the sensor's sampling frequency) and $N_W = 7$ is the number of days in a week. The temporal embeddings are thus shared among slots for the same time of the day and the same day of the week. Semantic temporal positional embeddings are helpful since traffic systems usually reflect the periodicity of human society. In addition, kindly note that all other baseline models [1], [3], [4], [32], [33], [34] also use such temporal features, so there is no unfairness. $\text{Linear}(\cdot)$ is a linear layer to reduce the hidden dimension. \mathbf{E} , \mathbf{T}^{TiD} , and \mathbf{T}^{DiW} are trainable parameters.

Embedding \mathbf{E} is vital for reducing the complexity of modeling the spatial correlations between time series. This is because attaching spatial embeddings plays a similar role to GCN in terms of solving the indistinguishability of samples [40], but with two primary advantages. On the one hand, it is more efficient than GCNs, which usually have $\mathcal{O}(N^2)$ complexity. On the other hand, it does not generate many additional network parameters than approaches based on variable-specific modeling [?], [20].

5.3 Hierarchical Encoder

Window Transformer Layer. Standard Transformer Layers [10] are designed based on the multi-head self-attention mechanism. As shown in Figure 3(a), it computes the attention among all input tokens. Therefore, each layer of the Transformer Layer has an infinite receptive field, and many works [9], [32], [33], [34] try to capture long-term dependencies based on such a feature.

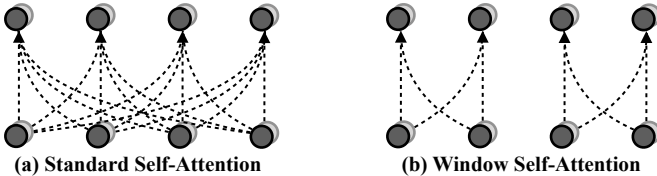


Fig. 3. Standard self-attention v.s. window self-attention.

However, the infinite receptive field makes the standard Transformer layers unable to generate multi-scale features [42]. Inspired by recent development in computer vision [42], we apply the window self-attention in HUTFormer to extract the hierarchical multi-scale features. An example of window self-attention with windows size 2 is

shown in Figure 3(b). Window self-attention forces calculating attention inside non-overlapping windows, thereby limiting the size of the receptive field. By replacing multi-head self-attention in standard Transformer layers [10] with the Window Multi-head Self-Attention (W-MSA), we present the window Transformer layer:

$$\begin{aligned} \mathbf{H}^{in'} &= \text{W-MSA}(\text{LN}(\mathbf{H}^{in})) + \mathbf{H}^{in}, \\ \mathbf{H}^{out} &= \text{MLP}(\text{LN}(\mathbf{H}^{in'})) + \mathbf{H}^{in'}, \end{aligned} \quad (3)$$

where $\text{LN}(\cdot)$ is the layer normalization, and $\text{MLP}(\cdot)$ is the multi-layer perceptron. $\mathbf{H}^{in} \in \mathbb{R}^{P \times d}$ and $\mathbf{H}^{out} \in \mathbb{R}^{P \times d}$ are the input and output sequences. P is the sequence length, and d is the hidden dimension. By limiting the receptive field size, the window transformer layer is the basis for extracting multi-scale features.

Segment Merging. To generate hierarchical multi-scale representations, we adopt segment merging, which reduces the number of tokens and increases the number of hidden dimensions as the network gets deeper. As illustrated in Figure 4, segment merging divides the token series into non-overlapping groups of size 2, and concatenates the features within each group.

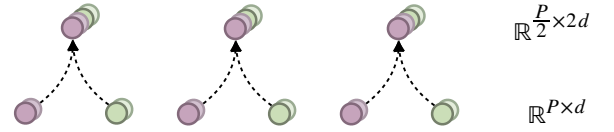


Fig. 4. An illustration of segment merging.

By combining the segment merging and window transformer layer, we get the basic block of the hierarchical encoder (*i.e.*, the blue block in Figure 2). Assuming $(\mathbf{H}^i)_{enc}^l \in \mathbb{R}^{P^l \times d^l}$ is the representation of time series i after block l ($l \geq 1$) of the encoder, the $(l+1)$ th block is computed as:

$$\begin{aligned} (\mathbf{H}^i)_{enc}^{l'} &= \text{SegmentMerging}((\mathbf{H}^i)_{enc}^l), \\ (\mathbf{H}^i)_{enc}^{l+1} &= \text{WindowTransformer}((\mathbf{H}^i)_{enc}^{l'}), \end{aligned} \quad (4)$$

where $(\mathbf{H}^i)_{enc}^{l+1} \in \mathbb{R}^{P^{l+1} \times d^{l+1}}$ is the representation of time series i after block $l+1$ of the encoder. $P^{l+1} = \frac{P^l}{2}$ is the number of tokens after $(l+1)$ th layer, and $d^{l+1} = 2d^{l+1}$ is the hidden dimension.

Prediction Layer. Assuming there are S blocks in the encoder, HUTFormer makes an intermediate prediction with a linear layer:

$$\hat{\mathbf{Y}}_{enc}^i = \text{Linear}\left(\parallel_{j=1}^S (\mathbf{H}_j^i)_{enc}^S\right), \quad (5)$$

where P^S is the number of tokens after the S th block. $\hat{\mathbf{Y}}^i \in \mathbb{R}^{T_f \times C}$ is the prediction of time series i . Considering the prediction from all N time series, $\hat{\mathbf{Y}}^{enc} \in \mathbb{R}^{T_f \times N \times C}$, we compute the Mean Absolute Error (MAE) as regression loss to train the hierarchical encoder:

$$\mathcal{L}_{enc} = \frac{1}{T_f N C} \sum_{j=1}^{T_f} \sum_{i=1}^N \sum_{k=1}^C |\hat{y}_{ijk}^{enc} - y_{ijk}|. \quad (6)$$

5.4 Hierarchical Decoder

Cross-Scale Transformer Layer. The hierarchical decoder aims to effectively utilize the multi-scale features, to fine-tune each segment of the intermediate prediction. However, as discussed in Section 5.1, the history and future sequence in traffic forecasting tasks are not aligned, making the feature sequences extracted by the encoder and the decoder cannot be directly superimposed. Therefore, we design a cross-scale attention mechanism to select and incorporate multi-scale features. Different from self-attention, cross-scale attention utilizes the representations of the decoder as *queries* to retrieve the multi-scale features from the encoder. For brevity, we denote $\mathbf{H}_{enc} \in \mathbb{R}^{P_{enc} \times d_{enc}}$ as the representation from the encoder and $\mathbf{H}_{dec} \in \mathbb{R}^{P_{dec} \times d_{dec}}$ as the corresponding representation from the decoder. Then, the Cross-scale Attention (CA) is computed as:

$$\text{CA}(\mathbf{H}_{enc}, \mathbf{H}_{dec}) = \text{Softmax}\left(\frac{\mathbf{H}_{dec}(\mathbf{H}_{enc}')^T}{\sqrt{d_{dec}}}\right)\mathbf{H}_{enc}', \quad (7)$$

$$\mathbf{H}_{enc}' = \text{Linear}(\mathbf{H}_{enc}),$$

The Linear(\cdot) layer is used to transform the hidden dimension from d_{enc} to d_{dec} . By replacing the multi-head self-attention with Multi-head Cross-scale Attention (MCA), we present the cross-scale Transformer layer as:

$$\mathbf{H}_{dec}^{in'} = \text{MCA}(\text{LN}(\mathbf{H}_{enc}^{in}, \mathbf{H}_{dec}^{in})) + \mathbf{H}_{dec}^{in}, \quad (8)$$

$$\mathbf{H}_{dec}^{out} = \text{MLP}(\text{LN}(\mathbf{H}_{dec}^{in'})) + \mathbf{H}_{dec}^{in'}$$

where \mathbf{H}_{enc}^{in} is the multi-scale feature from the encoder, and \mathbf{H}_{dec}^{in} is the input feature from the decoder. \mathbf{H}_{dec}^{out} is the output of the cross-scale Transformer layer.

Prediction Layer. Assuming $(\mathbf{H}_j^i)^S \in \mathbb{R}^{d_{dec}}$ is the representation of the decoder's last block (*i.e.*, the S th block) for j th segment of i th time series, HUTFormer makes the final prediction for each segment with a shared linear layer:

$$(\hat{\mathbf{Y}}_j^i)_{dec} = \text{Linear}((\mathbf{H}_j^i)^S_{dec}), \quad (9)$$

where $(\hat{\mathbf{Y}}_j^i)_{dec} \in \mathbb{R}^{LC}$ is the final prediction of segment j of time series i . Similar to the encoder, we consider the prediction from all P_{dec} segments ($P_{dec} \times L = T_f$) of all N time series, $\hat{\mathbf{Y}}^{dec} \in \mathbb{R}^{T_f \times N \times C}$, and compute the MAE loss to train the hierarchical decoder:

$$\mathcal{L}_{dec} = \frac{1}{T_f N C} \sum_{j=1}^{T_f} \sum_{i=1}^N \sum_{k=1}^C |\hat{\mathbf{Y}}_{ijk}^{dec} - \mathcal{Y}_{ijk}|. \quad (10)$$

Kindly note that the parameters of the encoder are fixed during this stage to serve as a pre-training model for extracting robust hierarchical multi-scale representations of traffic data.

6 EXPERIMENTS

In this section, we conduct extensive experiments on four real-world traffic datasets to validate the effectiveness of HUTFormer for long-term traffic forecasting. First, we introduce the experimental settings, including datasets, baselines, and implementation details. Then, we compare HUTFormer with other state-of-the-art traffic forecasting baselines and long-sequence time series forecasting baselines.

TABLE 2
Statistics of datasets.

Type	Dataset	# Samples	# Sensors	Sample Rate
Speed	METR-LA	34272	207	5 minutes
	PEMS-BAY	52116	325	5 minutes
Flow	PEMS04	16992	307	5 minutes
	PEMS08	17856	170	5 minutes

Furthermore, we conduct more experiments to evaluate the impact of important components and strategies, including the effectiveness of the hierarchical U-net structure, the input embedding strategy, and the two-stage training strategy.

6.1 Experimental Setting

Datasets. We conduct experiments on four commonly used traffic datasets, including two traffic speed datasets (METR-LA and PEMS-BAY) and two traffic flow datasets (PEMS04 and PEMS08). The statistical information is summarized in Table 2.

- **METR-LA** is a traffic speed dataset collected from loop-detectors located on the LA County road network [43]. It contains data of 207 selected sensors over a period of 4 months from Mar to Jun in 2012 [3]. The traffic information is recorded at the rate of every 5 minutes, and the total number of time slices is 34,272.
- **PEMS-BAY** is a traffic speed dataset collected from California Transportation Agencies (CalTrans) Performance Measurement System (PeMS) [44]. It contains data of 325 sensors in the Bay Area over a period of 6 months from Jan 1st 2017 to May 31th 2017 [3]. The traffic information is recorded at the rate of every 5 minutes, and the total number of time slices is 52,116.
- **PEMS04** is a traffic flow dataset also collected from CalTrans PeMS. It contains data of 307 sensors over a period of 2 months from Jan 1st 2018 to Feb 28th 2018 [30]. The traffic information is recorded at the rate of every 5 minutes, and the total number of time slices is 16,992.
- **PEMS08** is a public traffic flow dataset collected from CalTrans PeMS. Specifically, PEMS08 contains data of 170 sensors in San Bernardino over a period of 2 months from July 1st 2018 to Aug 31th 2018 [30]. The traffic information is recorded at the rate of every 5 minutes, and the total number of time slices is 17,856.

Baselines. On the one hand, we select six traffic forecasting baselines, including

- **DCRNN** [3] (Diffusion Convolutional Recurrent Neural Network) is one of the earliest works for STGNN-based traffic forecasting, which replaces the fully connected layer in GRU [16] by diffusion convolutional layer to form a Diffusion Convolutional Gated Recurrent Unit (DCGRU).
- **Graph WaveNet** [4] is a traffic forecasting model, which stacks gated temporal convolutional layer and GCN layer by layer to jointly capture the spatial and temporal dependencies.
- **MTGNN** [24] is a traffic forecasting model, which extends Graph WaveNet through the mix-hop propagation layer in the spatial module, the dilated inception

layer in the temporal module, and a delicate graph learning layer.

- **STID** [40] is a simple but effective baseline for traffic forecasting, which identifies the indistinguishability of samples in both spatial and temporal dimensions as a key bottleneck, and addresses the indistinguishability by attaching spatial and temporal identities.
- **STEP** [8] is a traffic forecasting model, which enhances existing STGNNs with the help of a time series pre-training model. It significantly extends the length of historical data.
- **D²STGNN** [1]: D²STGNN is a state-of-the-art traffic forecasting model, which identifies the diffusion process and inherent process in traffic data, and further decouples them for better modeling.

On the other hand, we also select six long-sequence forecasting baselines, including

- **HI** [45]: HI (Historical Inertia) is a basic baseline for long-sequence time series forecasting problems, which directly takes the most recent time steps in the input as output.
- **DLinear** [35]: DLinear is a simple but effective long-sequence time series forecasting model, which decomposes the time series into a trend and a remainder series and employs two one-layer linear networks to model these two series.
- **Informer** [9]: Informer is a model for long-sequence time series forecasting, which designs a ProbSparse self-attention mechanism and distilling operation to handle the challenges of the quadratic complexity in the standard Transformer. Also, it carefully designs a generative decoder to alleviate the limitation of standard encoder-decoder architecture.
- **Autoformer** [32]: Autoformer is a model for long-sequence time series forecasting, which is proposed as a decomposition architecture by embedding the series decomposition block as an inner operator. Besides, it designs an efficient Auto-Correlation mechanism to conduct dependencies discovery and information aggregation at the series level.
- **FEDformer** [33]: FEDformer [33] is a frequency-enhance Transformer for long-sequence time series forecasting problems. It proposes an attention mechanism with low-rank approximation in frequency and a mixture of experts decomposition to control the distribution shifting.
- **Pyraformer** [34]: Pyraformer [34] is a pyramidal attention-based model for long-sequence time series forecasting. Pyramidal attention can effectively describe short and long temporal dependencies with low time and space complexity.

Metrics. In this paper, we evaluate the performances of all baselines by Mean Absolute Error (MAE) and Mean Absolute Percentage Error (MAPE) metrics. First, the MAE metric reflects the absolute prediction error, but is affected by the units of the dataset. For example, traffic speed datasets usually take values between 0km/h and 70km/h, while traffic flow datasets usually take values between 0 and hundreds. Thus, we also adopt MAPE, which can eliminate the impact of data units and reflects the relative error,

helping to understand the accuracy more intuitively.

Implementation. For all datasets, we use historical $T_p = 288$ time steps (*i.e.*, one day) to predict future $T_f = 288$ time steps. For HUTFormer, we set the segment length L to 12, and the number of segments $P = 24$ ($L \times P = 288$). We set the window size to 3. We set the hidden dimension of temporal embedding \mathbf{T}^{TiD} to 8, while others d to 32. The depth of HUTFormer is set to 4. For baselines, we adopt the default settings in their paper. Moreover, as discussed before, STGNNs can not directly handle the long-term traffic forecasting task due to their high complexity. Therefore, we first apply the segment embedding to reduce the length of input tokens for them¹.

Optimization Settings. For both encoding and decoding stages, we apply the optimization settings in Tabel 3. Specifically, we adopt Adam as our optimizer, and set learning rate and weight decay to 0.0005 and 0.0001, respectively. The batch size is set to 64. In addition, we use a learning rate scheduler, MultiStepLR, which adjusts the learning rate at epochs 1, 40, 80, and 120 with gamma 0.5. Moreover, the gradient clip is set to 5. All the experiments in Section 6 are running on an Intel(R) Xeon(R) Gold 5217 CPU @ 3.00GHz, 128G RAM computing server, equipped with RTX 3090 graphics cards.

TABLE 3
Optimization settings.

config	value
optimizer	Adam
learning rate	0.0005
batch size	64
weight decay	0.0001
learning rate schedule	MultiStepLR
milestones	[1, 40, 80, 120]
gamma	0.5
gradient clip	5

6.2 Main Results

Settings. We follow the dataset division in previous works. Specifically, for traffic speed datasets (METR-LA and PEMS-BAY), we use 70%, 10%, and 20% of the data for training, validating, and testing, respectively. For traffic flow datasets (PEMS04 and PEMS08), we use 60%, 20%, and 20% of data for training, validating, and testing, respectively. We compare the performance at 1, 4, 8, 12, 16, and 24 hours (horizon 12, 48, 96, 144, 192, and 288) of forecasting on the MAE and MAPE metrics.

Results. The results of traffic speed and traffic flow forecasting are shown in Table 4 and 6, respectively. In general, HUTFormer consistently outperforms all baselines, indicating its effectiveness.

Long-sequence forecasting models do not perform well on traffic forecasting tasks. We conjecture that the main reason is that these models do not fit the characteristics of traffic data. *First*, there exist strong correlations between the time series of traffic data. For example, due to the constraint of road networks, time series from adjacent sensors or

1. Methods implemented with segment embeddings are marked with *.

TABLE 4
Long-term traffic forecasting on traffic speed datasets METR-LA and PEMS-BAY.

Data	Methods	@Horizon 12		@Horizon 48		@Horizon 96		@Horizon 144		@Horizon 192		@Horizon 288		
		MAE	MAPE	MAE	MAPE	MAE	MAPE	MAE	MAPE	MAE	MAPE	MAE	MAPE	
METR-LA	HI	10.44	23.21%	10.42	23.19%	10.43	23.23%	10.43	23.32%	10.40	23.34%	10.22	22.81%	
	DLinear	7.61	16.19%	12.86	23.79%	12.99	23.11%	12.90	23.48%	12.89	23.15%	13.07	23.33%	
	Informer	4.65	15.52%	4.86	16.54%	4.98	17.16%	5.07	17.41%	5.07	17.30%	5.06	17.14%	
	Autoformer	7.23	19.25%	7.27	19.73%	7.45	20.23%	7.83	21.49%	7.74	20.98%	8.41	22.43%	
	FEDformer	8.78	22.29%	9.11	22.69%	9.12	22.75%	9.54	24.18%	9.81	24.76%	10.13	25.56%	
	Pyraformer	4.22	12.84%	4.55	14.93%	4.75	15.81%	4.80	15.89%	4.81	15.68%	4.62	14.79%	
	DCRNN*	4.07	12.74%	4.39	14.08%	4.44	14.02%	4.46	14.16%	4.51	14.41%	4.71	15.59%	
	GWNet*	3.87	12.18%	4.19	13.60%	4.25	13.62%	4.42	14.56%	4.58	15.40%	4.51	15.09%	
	MTGNN*	4.01	12.31%	4.31	13.84%	4.53	14.85%	4.59	14.77%	4.57	15.18%	4.75	15.93%	
	STID	3.84	12.17%	4.13	14.11%	4.04	13.05%	4.11	13.65%	4.15	14.07%	4.17	13.83%	
	STEP*	3.74	11.60%	4.14	13.24%	4.22	13.52%	4.38	14.07%	4.34	13.96%	4.43	14.42%	
	D ² STGNN*	3.71	11.24%	3.96	12.84%	3.99	13.26%	4.05	13.17%	4.05	13.36%	4.09	12.78%	
	HUTFormer	3.59	10.93%	3.77	11.88%	3.79	11.86%	3.80	12.08%	3.82	12.18%	3.84	12.28%	
	PEMS-BAY	HI	3.37	7.84%	3.36	7.80%	3.36	7.77%	3.36	7.76%	3.36	7.74%	3.38	7.79%
		DLinear	2.70	6.28%	3.14	7.75%	3.13	7.77%	3.15	7.76%	3.15	7.78%	3.23	7.90%
Informer		2.77	6.65%	2.80	6.88%	2.84	7.06%	2.83	7.07%	2.82	6.98%	2.92	7.16%	
Autoformer		3.15	7.48%	3.24	7.85%	3.30	8.00%	3.37	8.10%	3.39	8.15%	4.35	11.25%	
FEDformer		3.04	7.55%	3.14	7.61%	3.13	7.58%	3.32	8.00%	3.42	8.45%	3.67	9.33%	
Pyraformer		2.53	6.21%	2.71	6.72%	2.64	6.39%	2.74	6.65%	2.75	6.68%	2.77	6.81%	
DCRNN*		2.18	5.49%	2.52	6.49%	2.54	6.43%	2.66	6.79%	2.67	6.80%	2.66	6.62%	
GWNet*		2.01	5.11%	2.35	5.91%	2.40	5.98%	2.47	6.35%	2.46	6.24%	2.46	6.09%	
MTGNN*		2.17	5.40%	2.45	6.11%	2.51	6.04%	2.52	6.13%	2.57	6.19%	2.70	6.40%	
STID		2.02	5.02%	2.29	5.66%	2.32	5.69%	2.33	5.72%	2.32	5.67%	2.38	5.81%	
STEP*		2.00	4.94%	2.33	5.93%	2.38	6.05%	2.44	6.26%	2.45	6.24%	2.54	6.41%	
D ² STGNN*		2.04	4.97%	2.26	5.44%	2.29	5.60%	2.34	5.55%	2.31	5.50%	2.38	5.64%	
HUTFormer		1.93	4.62%	2.18	5.16%	2.21	5.24%	2.22	5.24%	2.23	5.25%	2.28	5.35%	

from similar geographical functional areas may be more similar [19]. Understanding and exploiting the correlations between time series is essential for traffic forecasting. However, long-sequence forecasting models are usually not concerned with such spatial dependencies. *Second*, as discussed in Section 1, the long-term traffic forecasting task requires exploiting multi-scale representations to capture the complex dynamics of traffic data. However, most long-term sequence forecasting models mainly focus on capturing global dependencies based on self-attention mechanisms. For example, Informer [9] optimizes the efficiency of the original self-attention mechanism through the ProbSparse mechanism. Autoformer [32] conducts the dependencies discovery at the series level. They can not generate and utilize multi-scale representations of traffic data. In summary, the above-mentioned uniqueness of long-term traffic forecasting tasks significantly affects the effectiveness of long-sequence forecasting models.

Compared to long-sequence forecasting models, traffic forecasting models achieve better performance. This is mainly because they model correlations between time series with the help of graph convolution. Most of them [1], [3], [4], [8], [24] utilize diffusion convolution, a variant of graph convolution, to model the diffusion process at each time step. However, there is no free lunch. The graph convolution brings a high complexity [8]. As mentioned earlier, we had to implement these models with the segment embedding in HUTFormer to reduce the length of input tokens to make them runnable. Kindly note that although the latest

baseline STEP [8] can handle long-term historical data, it still requires a downstream STGNN as the backend, which can only make short-term future predictions. In summary, these models only focus on short-term traffic forecasting and do not consider the uniqueness of long-term traffic forecasting, *i.e.*, exploiting multi-scale representations.

Compared to all baselines, HUTFormer achieves state-of-the-art performances by sufficiently addressing the issues of long-term traffic forecasting tasks. Specifically, on the one hand, HUTFormer efficiently handles the correlations between long-term time series with spatial-temporal positional encoding and segment embedding. On the other hand, HUTFormer effectively generates and utilizes multi-scale representations based on the hierarchical U-net.

6.3 Efficiency

In this section, we conduct more experiments to evaluate the efficiency of the HUTFormer variants in Section 6.5. We conduct experiments with a single NVIDIA V100 graphics card with 32GB memory, and report the GPU memory usage and running time. Specifically, for the two-stage training variants, we report the largest GPU memory usage of the two stages and report the sum of the running time in the encoding and decoding stages. We conduct experiments on the METR-LA dataset.

The results are shown in Figure 5. First, we can see that removing the segment embedding (*i.e.*, *w/o SE*) will significantly increase the computational complexity, and require more GPU memory. Second, compared with applying GCN,

TABLE 5
Long-term traffic forecasting on traffic flow datasets PEMS04 and PEMS08.

Data	Methods	@Horizon 12		@Horizon 48		@Horizon 96		@Horizon 144		@Horizon 192		@Horizon 288	
		MAE	MAPE	MAE	MAPE	MAE	MAPE	MAE	MAPE	MAE	MAPE	MAE	MAPE
PEMS04	HI	41.73	28.46%	41.16	28.61%	41.38	28.62%	41.28	28.42%	30.99	27.34%	39.58	26.49%
	DLinear	27.29	19.83%	37.20	26.51%	37.50	26.78%	37.57	26.87%	37.17	25.27%	36.87	25.21%
	Informer	25.94	17.56%	25.72	18.05%	25.60	18.27%	25.98	17.81%	26.42	17.67%	27.42	18.57%
	Autoformer	29.94	28.00%	31.30	27.41%	31.47	27.73%	31.95	27.89%	32.03	28.03%	33.34	29.82%
	FEDformer	34.94	34.33%	32.24	37.23%	33.90	34.33%	35.12	41.26%	35.16	34.08%	41.83	51.01%
	Pyraformer	23.40	17.18%	25.40	18.80%	26.45	19.89%	26.22	19.01%	26.51	19.18%	26.58	20.57%
	DCRNN*	22.25	16.59%	24.42	18.89%	25.20	19.17%	26.31	19.61%	27.32	19.74%	28.04	21.02%
	GWNet*	22.24	16.51%	23.50	18.29%	24.08	18.07%	24.85	18.21%	25.83	18.98%	31.17	21.00%
	MTGNN*	21.75	15.93%	23.04	17.81%	24.33	17.80%	25.56	17.68%	25.80	17.85%	26.78	20.64%
	STID	21.01	15.24%	22.77	16.61%	23.39	16.87%	24.06	17.08%	24.43	17.22%	25.19	17.49%
	STEP*	20.82	15.56%	22.23	17.11%	22.87	17.21%	24.46	17.97%	24.89	17.40%	26.18	18.47%
	D ² STGNN*	21.55	16.03%	22.98	17.04%	24.16	17.57%	24.50	17.93%	24.59	17.19%	24.79	17.97%
	HUTFormer	19.61	13.59%	21.54	14.95%	21.96	15.22%	22.66	15.30%	23.10	15.35%	23.43	15.71%
PEMS08	HI	37.33	25.01%	37.31	25.07%	37.23	25.05%	37.09	25.02%	36.94	24.98%	36.40	24.76%
	DLinear	22.91	17.23%	34.13	24.15%	34.34	25.54%	34.44	23.80%	34.52	23.91%	35.11	23.71%
	Informer	24.55	14.76%	24.80	15.03%	24.72	15.03%	25.07	15.11%	24.82	14.91%	25.09	15.61%
	Autoformer	31.36	25.44%	32.29	27.13%	33.19	27.45%	32.98	26.15%	33.57	25.78%	36.75	28.82%
	FEDformer	24.62	20.01%	26.76	21.85%	28.56	23.02%	30.33	24.47%	29.11	23.14%	29.91	24.47%
	Pyraformer	21.92	14.43%	23.00	14.70%	23.80	15.46%	24.45	16.88%	24.34	16.17%	22.71	14.79%
	DCRNN*	18.64	13.47%	20.42	14.92%	20.97	15.11%	21.63	15.51%	22.45	16.23%	22.95	16.72%
	GWNet*	17.07	11.57%	19.55	11.93%	20.38	14.33%	20.49	14.82%	20.00	14.68%	20.29	15.20%
	MTGNN*	17.75	12.61%	19.27	13.35%	19.99	13.85%	20.68	15.00%	20.95	14.65%	22.16	15.68%
	STID	16.40	11.42%	18.53	13.26%	19.17	13.66%	19.59	13.78%	19.59	14.03%	20.23	15.35%
	STEP*	16.67	11.34%	19.05	14.00%	19.74	14.74%	20.15	14.88%	19.80	14.84%	20.37	15.54%
	D ² STGNN*	17.27	11.47%	18.45	12.35%	18.97	12.63%	19.33	12.81%	19.09	12.34%	19.55	12.93%
	HUTFormer	15.18	10.09%	16.72	11.26%	17.23	11.55%	17.59	11.74%	17.83	11.84%	18.44	12.20%

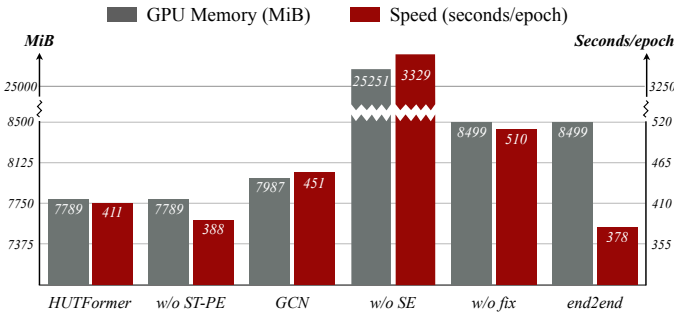


Fig. 5. Efficiency Study.

HUTFormer is more efficient and effective by leveraging the spatial-temporal positional encoding, which does not increase much complexity.

6.4 Generalization

The ability of HUTFormer to generate and utilize multi-scale features should also be effective in many non-traffic data, since the multi-scale features widely exists in many domains. In order to verify the generalization of HUTFormer, in this part, we compare HUTFormer with more latest Transformer-based long time series forecasting models [46], [47] based on three commonly used long-sequence prediction datasets, ETTh1, ETTm1, and Weather. The details of Crossformer [46] and Triformer [47] as well as the three datasets are neglected for simplicity. Interest readers can

refer to their papers [46], [47]. We use the same setting as the other datasets in our paper. As shown in the table 6.2, HUTFormer still outperforms these models on these datasets, which further verifies the effectiveness and generalization of HUTFormer.

6.5 Ablation Study

In this subsection, we conduct more experiments to evaluate the impact of some important components and strategies. Specifically, we evaluate from three aspects, including the effectiveness of the hierarchical U-net structure, the input embedding strategy, and the two-stage training strategy. Due to space limitations, we only present the results on METR-LA datasets in Table 7.

The hierarchical U-net structure is designed to generate and exploit multi-scale features. Specifically, the encoder combines window self-attention and segment merging to generate multi-scale features, while the decoder primarily utilizes extracted features based on cross-scale attention. Therefore, to evaluate their effectiveness, we set up three variants. First, we replace the decoder with a simple concatenation, named *HUTFormer concat*. The concatenation of features from different scales naturally preserves all information. Second, we set *HUTFormer w/o decoder* to remove the decoder and use the intermediate prediction as the final prediction. The above two variants are used to demonstrate that exploiting multi-scale features is a non-trivial challenge and our hierarchical decoder is effective. Third, we set *HUTFormer w/o hierarchy* to further remove

TABLE 6
Experiments on ETTh1, ETTm1, and Weather datasets.

Data	Methods	@Horizon 12		@Horizon 48		@Horizon 96		@Horizon 144		@Horizon 192		@Horizon 288	
		MAE	MSE	MAE	MSE	MAE	MSE	MAE	MSE	MAE	MSE	MAE	MSE
ETTh1	Informer	0.72	1.01	0.79	1.16	0.87	1.34	0.96	1.61	0.97	1.66	0.97	1.68
	Autoformer	0.54	0.56	0.56	0.61	0.57	0.64	0.58	0.66	0.60	0.69	0.68	0.85
	FEDformer	0.52	0.50	0.54	0.55	0.56	0.57	0.57	0.60	0.58	0.62	0.64	0.73
	Pyraformer	0.56	0.63	0.57	0.64	0.65	0.79	0.74	0.92	0.76	1.03	0.79	1.09
	Triformer	0.46	0.42	0.53	0.54	0.56	0.59	0.57	0.60	0.58	0.61	0.60	0.68
	Crossformer	0.45	0.40	0.50	0.49	0.54	0.57	0.55	0.60	0.56	0.61	0.58	0.63
	HUTFormer	0.41	0.36	0.46	0.43	0.49	0.47	0.51	0.50	0.52	0.53	0.54	0.56
ETTM1	Informer	0.53	0.59	0.60	0.67	0.63	0.74	0.68	0.85	0.72	0.91	0.74	0.95
	Autoformer	0.49	0.56	0.55	0.58	0.57	0.62	0.59	0.67	0.59	0.69	0.63	0.84
	FEDformer	0.46	0.42	0.49	0.49	0.52	0.53	0.54	0.58	0.55	0.60	0.59	0.66
	Pyraformer	0.50	0.51	0.54	0.57	0.57	0.68	0.59	0.70	0.61	0.77	0.66	0.84
	Triformer	0.33	0.25	0.39	0.35	0.40	0.38	0.45	0.45	0.46	0.45	0.48	0.48
	Crossformer	0.35	0.27	0.47	0.45	0.49	0.46	0.54	0.55	0.56	0.58	0.57	0.59
	HUTFormer	0.31	0.23	0.40	0.36	0.40	0.38	0.46	0.44	0.46	0.45	0.47	0.46
Weather	Informer	0.34	0.27	0.38	0.36	0.40	0.38	0.43	0.42	0.45	0.46	0.45	0.48
	Autoformer	0.32	0.24	0.34	0.28	0.36	0.31	0.38	0.34	0.40	0.37	0.43	0.42
	FEDformer	0.29	0.21	0.30	0.24	0.32	0.27	0.34	0.30	0.35	0.32	0.39	0.39
	Pyraformer	0.28	0.23	0.31	0.29	0.34	0.32	0.35	0.33	0.45	0.48	0.52	0.60
	Triformer	0.30	0.23	0.43	0.45	0.47	0.54	0.47	0.56	0.51	0.59	0.52	0.64
	Crossformer	0.18	0.15	0.26	0.20	0.30	0.24	0.32	0.27	0.35	0.32	0.37	0.37
	HUTFormer	0.18	0.15	0.23	0.19	0.26	0.23	0.28	0.24	0.31	0.30	0.33	0.32

TABLE 7
Ablation study on the METR-LA dataset.

Variants	@Horizon 12		@Horizon 48		@Horizon 96		@Horizon 144		@Horizon 192		@Horizon 288	
	MAE	MAPE	MAE	MAPE	MAE	MAPE	MAE	MAPE	MAE	MAPE	MAE	MAPE
HUTFormer	3.59	10.93%	3.77	11.88%	3.79	11.86%	3.80	12.08%	3.82	12.18%	3.84	12.28%
<i>concat</i>	3.86	12.16%	3.98	13.23%	4.01	13.36%	4.01	13.36%	4.05	13.41%	4.08	13.65%
<i>w/o decoder</i>	3.80	11.94%	3.85	12.33%	3.90	12.64%	3.88	12.91%	3.96	12.91%	3.97	12.93%
<i>w/o hierarchy</i>	3.90	12.56%	3.97	12.85%	3.96	12.86%	3.98	12.88%	3.98	12.92%	4.12	13.48%
<i>w/o ST-PE</i>	4.11	12.68%	4.78	15.80%	4.90	16.44%	5.00	16.81%	5.13	17.47%	5.25	17.56%
<i>GCN</i>	3.79	11.87%	4.23	14.14%	4.28	14.32%	4.30	14.21%	4.32	14.28%	4.35	14.40%
<i>w/o SE</i>	3.76	11.83%	3.86	12.39%	3.85	12.35%	3.91	12.73%	3.92	12.75%	4.03	13.12%
<i>end2end</i>	3.72	11.60%	3.95	12.59%	3.97	12.83%	3.95	12.58%	3.95	12.58%	4.00	12.73%
<i>w/o fix</i>	3.64	11.28%	3.85	12.11%	3.88	12.49%	3.90	12.40%	3.93	12.57%	3.91	12.57%

segment merging and replace the window Transformer layer with a standard Transformer layer, to evaluate the effectiveness of hierarchical multi-scale representations. As shown in Table 4, *HUTFormer* significantly outperforms *HUTFormer concat* and *HUTFormer w/o decoder*, which shows that it is not an easy task to utilize the multi-scale features, and also validates the effectiveness of our decoder. In addition, the results of *HUTFormer w/o hierarchy* show that hierarchical multi-scale features are crucial for accurate long-term traffic forecasting. The above results show that generating and utilizing hierarchical multi-scale features is important, and the designed hierarchical U-net structure is effective.

The input embedding strategy aims to address the complexity issue from both spatial and temporal dimensions. Specifically, it consists of a Segment Embedding (SE) and a Spatial-Temporal Positional Encoding (ST-PE). To ver-

ify their effectiveness, we set up three variants. First, we set *HUTFormer w/o ST-PE*, which replaces the ST-PE with standard learnable positional encoding. Second, we set *HUTFormer GCN*, which replaces the spatial embeddings in ST-PE with graph convolution [4]. Third, we remove the segment embedding to get *HUTFormer w/o SE*. As shown in Table 7, without ST-PE, the performance of *HUTFormer* decreases significantly. This is because modeling the correlations between time series is the basis of traffic forecasting. In addition, we can see that the ST-PE strategy is significantly better than performing graph convolution, indicating the superiority of ST-PE. Moreover, removing segment embedding not only leads to a significant decrease in performance but also increases the complexity due to the increased sequence length. These results indicate the effectiveness of the spatial-temporal positional encoding and segment merging.

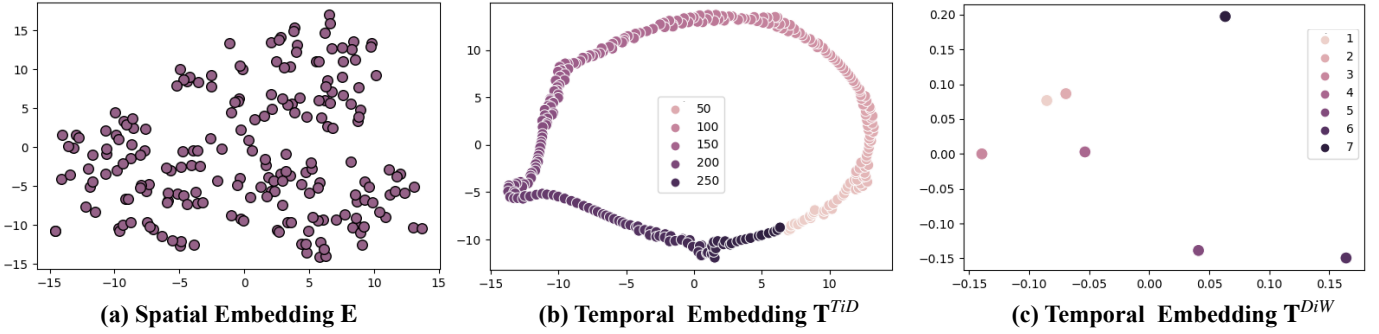


Fig. 6. Visualization of the spatial and temporal embeddings.

Finally, we evaluate the two-stage training strategy of HUTFormer. To this end, we set two variants. First, we set *HUTFormer end2end*, which trains the HUTFormer in an end-to-end strategy. Second, we set *HUTFormer w/o fix*, which does not fix the parameter of the encoder when training the decoder. The results in Table 7 show that either the end-to-end strategy or the strategy without fixing the encoder leads to insufficient optimization and significant performance degradation. In addition, both strategies require more memory. In contrast, our two-stage strategy achieves the best performance and efficiency simultaneously.

6.6 Hyper-parameter Study

In this subsection, we conduct experiments to study the impact of two key hyper-parameters: segment size and window size. We conduct experiments on the METR-LA dataset and report the MAE at horizon 288. Moreover, we report the training speed of the encoder, since these hyper-parameters mainly affect the encoder. As shown in Figure 7(a), the segment size $L = 12$ achieves the best performance. Smaller segments cannot provide robust semantics, while larger segments ignore more local details. In addition, we can see that as the segment size increases, the encoder runs faster (seconds/epoch). Kindly note that changing the segment size may change the depth of the HUTFormer to ensure that the receptive field covers the entire sequence. The impact of the window size is shown in Figure 7(b), where larger window sizes perform worse. This is because the ability to extract multi-scale features is weakened as the window size increases. Moreover, the efficiency of HUTFormer will also decrease [42] on larger window sizes.

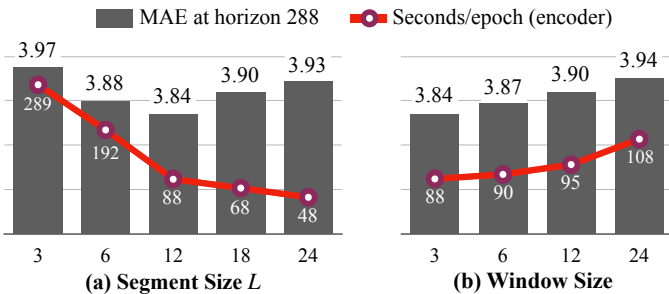


Fig. 7. Hyper-parameter study.

6.7 Visualization

6.7.1 Spatial-Temporal Positional Encoding

To further understand the HUTFormer in modeling the correlations between multiple time series in traffic data, we analyze the spatial-temporal positional encoding layer. Modeling correlations between multiple time series have been widely discussed in multivariate time series forecasting [4], [8], [24]. Previous works usually utilize Graph Convolution Networks (GCN), which conduct message passing in a pre-defined graph. GCN is a powerful model, but it has high complexity of $\mathcal{O}(N^2)$. Very recent works, STID [40] and ST-Norm [41], identify that graph convolution in multivariate time series forecasting is essentially used for addressing the indistinguishability of samples on the spatial dimension. Based on such an observation, STID proposes a simple but effective baseline of attaching spatial and temporal identities, achieving a similar performance of GCN but high efficiency. The Spatial-Temporal Positional Encoding (ST-PE) is designed based on such an idea [40].

The ST-PE contains three learnable positional embeddings, $\mathbf{E} \in \mathbb{R}^{N \times d}$, $\mathbf{T}^{TiD} \in \mathbb{R}^{N_D \times d}$ and $\mathbf{T}^{DiW} \in \mathbb{R}^{N_W \times d}$, where N is the number of time series, N_D is the number of time slots of a day (determined by the sensor’s sampling frequency), and $N_W = 7$ is the number of days in a week. We utilize t-SNE [14] to visualize these three embedding matrices. Kindly note that \mathbf{T}^{DiW} only have 7 embeddings, which is significantly less than the hidden dimension 32, making it hard to get correct visualizations. Therefore, we additionally train a HUTFormer with the embedding size of \mathbf{T}^{DiW} to 2 to get a more accurate visualization.

The results are shown in Figure 6. First, as shown in Figure 6(a), the spatial embeddings are likely to cluster. For example, traffic conditions observed by sensors that are connected or have similar geographical functionality are more likely to be similar. However, it is not as apparent as in the results in STID [40]. We conjecture this is because the impact of the indistinguishability of the samples becomes weaker as the length of the historical data increases. Second, Figure 6(b) shows the embeddings of 288 time slots, where the daily periodicity is very obvious. Third, Figure 6(c) visualizes the embeddings of each day in a week, where weekdays are closer and weekends’ are different.

6.7.2 Prediction Visualization

In order to further intuitively evaluate HUTFormer, in this subsection, we visualize the prediction of HUTFormer and

other baselines on the METR-LA dataset. Specifically, we select sensor 12 and displayed its data from June 05th, 2012 to June 06th, 2012 (located in the test dataset). The forecasting results of Autoformer [32], Graph WaveNet [4], HUTFormer w/o hierarchy, and HUTFormer are shown in Figure 8. First, Autoformer performs the worst, since it does not fit the characteristics of traffic data as discussed in Section 6.2. Graph WaveNet and HUTFormer w/o hierarchy perform well on smooth periods but fail to accurately capture the sudden change when traffic congestion occurs. In contrast, benefiting from exploiting multi-scale representations of traffic data, HUTFormer performs better in both smooth periods and sudden changes.

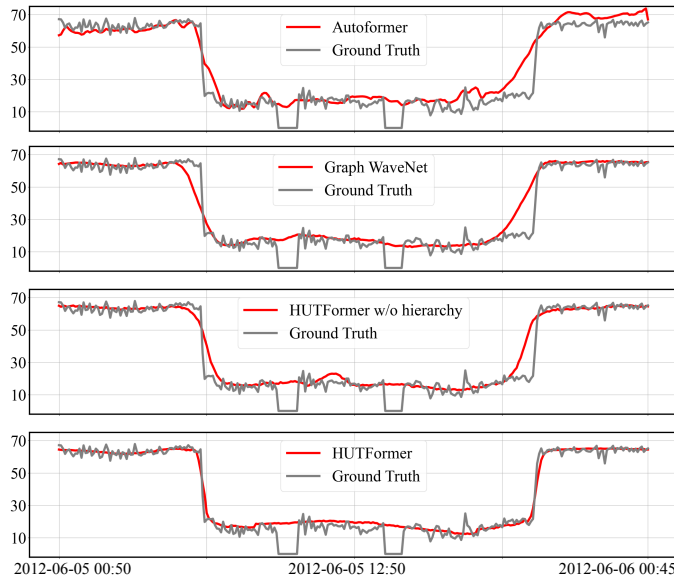


Fig. 8. Visualization of prediction results of HUTFormer and some baseline models.

7 CONCLUSIONS

In this paper, we make the first attempt to explore the long-term traffic forecasting problem. To this end, we reveal its unique challenges in exploiting the multi-scale representations of traffic data, and propose a novel *Hierarchical U-net Transformer* (HUTFormer) to efficiently and effectively address them. The HUTFormer mainly consists of a hierarchical encoder and decoder. On the one hand, the hierarchical encoder generates multi-scale representations based on the window self-attention mechanism and segment merging. On the other hand, the hierarchical decoder effectively utilizes the extracted multi-scale features based on the cross-scale attention mechanism. In addition, HUTFormer adopts segment embedding and spatial-temporal positional encoding as the input embedding strategy to address the complexity issue. Extensive experiments on four commonly used traffic datasets show that the proposed HUTFormer significantly outperforms state-of-the-art traffic forecasting and long-sequence time series forecasting baselines.

ACKNOWLEDGMENTS

This work is also supported by the Youth Innovation Promotion Association CAS No.2023112. In addition, Zhao Zhang

is supported by the China Postdoctoral Science Foundation under Grant No. 2021M703273.

REFERENCES

- [1] Z. Shao, Z. Zhang, W. Wei, F. Wang, Y. Xu, X. Cao, and C. S. Jensen, "Decoupled dynamic spatial-temporal graph neural network for traffic forecasting," *Proc. VLDB Endow.*, vol. 15, no. 11, pp. 2733–2746, 2022.
- [2] G. Jin, Y. Liang, Y. Fang, J. Huang, J. Zhang, and Y. Zheng, "Spatio-temporal graph neural networks for predictive learning in urban computing: A survey," *arXiv preprint arXiv:2303.14483*, 2023.
- [3] Y. Li, R. Yu, C. Shahabi, and Y. Liu, "Diffusion convolutional recurrent neural network: Data-driven traffic forecasting," in *6th International Conference on Learning Representations, ICLR 2018, Vancouver, BC, Canada, April 30 - May 3, 2018, Conference Track Proceedings*. OpenReview.net, 2018.
- [4] Z. Wu, S. Pan, G. Long, J. Jiang, and C. Zhang, "Graph wavenet for deep spatial-temporal graph modeling," in *Proceedings of the Twenty-Eighth International Joint Conference on Artificial Intelligence, IJCAI 2019, Macao, China, August 10-16, 2019*. ijcai.org, 2019, pp. 1907–1913.
- [5] G. Jin, F. Li, J. Zhang, M. Wang, and J. Huang, "Automated dilated spatio-temporal synchronous graph modeling for traffic prediction," *IEEE Transactions on Intelligent Transportation Systems*, 2022.
- [6] M. Defferrard, X. Bresson, and P. Vandergheynst, "Convolutional neural networks on graphs with fast localized spectral filtering," in *Advances in Neural Information Processing Systems 29: Annual Conference on Neural Information Processing Systems 2016, December 5-10, 2016, Barcelona, Spain*, D. D. Lee, M. Sugiyama, U. von Luxburg, I. Guyon, and R. Garnett, Eds., pp. 3837–3845.
- [7] T. N. Kipf and M. Welling, "Semi-supervised classification with graph convolutional networks," in *5th International Conference on Learning Representations, ICLR 2017, Toulon, France, April 24-26, 2017, Conference Track Proceedings*. OpenReview.net, 2017.
- [8] Z. Shao, Z. Zhang, F. Wang, and Y. Xu, "Pre-training enhanced spatial-temporal graph neural network for multivariate time series forecasting," in *KDD '22: The 28th ACM SIGKDD Conference on Knowledge Discovery and Data Mining, Washington, DC, USA, August 14 - 18, 2022*. ACM, 2022, pp. 1567–1577.
- [9] H. Zhou, S. Zhang, J. Peng, S. Zhang, J. Li, H. Xiong, and W. Zhang, "Informer: Beyond efficient transformer for long sequence time-series forecasting," in *Thirty-Fifth AAAI Conference on Artificial Intelligence, AAAI 2021, Thirty-Third Conference on Innovative Applications of Artificial Intelligence, IAAI 2021, The Eleventh Symposium on Educational Advances in Artificial Intelligence, EAAI 2021, Virtual Event, February 2-9, 2021*. AAAI Press, 2021, pp. 11 106–11 115.
- [10] A. Vaswani, N. Shazeer, N. Parmar, J. Uszkoreit, L. Jones, A. N. Gomez, L. Kaiser, and I. Polosukhin, "Attention is all you need," in *Advances in Neural Information Processing Systems 30: Annual Conference on Neural Information Processing Systems 2017, December 4-9, 2017, Long Beach, CA, USA, 2017*, pp. 5998–6008.
- [11] T. Lin, P. Dollár, R. B. Girshick, K. He, B. Hariharan, and S. J. Belongie, "Feature pyramid networks for object detection," in *2017 IEEE Conference on Computer Vision and Pattern Recognition, CVPR 2017, Honolulu, HI, USA, July 21-26, 2017*. IEEE Computer Society, 2017, pp. 936–944.
- [12] O. Ronneberger, P. Fischer, and T. Brox, "U-net: Convolutional networks for biomedical image segmentation," in *Medical Image Computing and Computer-Assisted Intervention - MICCAI 2015 - 18th International Conference Munich, Germany, October 5 - 9, 2015, Proceedings, Part III*, vol. 9351. Springer, 2015, pp. 234–241.
- [13] K. He, X. Zhang, S. Ren, and J. Sun, "Deep residual learning for image recognition," in *2016 IEEE Conference on Computer Vision and Pattern Recognition, CVPR 2016, Las Vegas, NV, USA, June 27-30, 2016*. IEEE Computer Society, 2016, pp. 770–778.
- [14] E. Cascetta, *Transportation systems engineering: theory and methods*. Springer Science & Business Media, 2013, vol. 49.
- [15] S. V. Kumar and L. Vanajakshi, "Short-term traffic flow prediction using seasonal arima model with limited input data," *European Transport Research Review*, vol. 7, no. 3, pp. 1–9, 2015.

- [16] K. Cho, B. van Merriënboer, D. Bahdanau, and Y. Bengio, "On the properties of neural machine translation: Encoder-decoder approaches," in *Proceedings of SSST@EMNLP 2014, Eighth Workshop on Syntax, Semantics and Structure in Statistical Translation, Doha, Qatar, 25 October 2014*. Association for Computational Linguistics, 2014, pp. 103–111.
- [17] I. Sutskever, O. Vinyals, and Q. V. Le, "Sequence to sequence learning with neural networks," in *Advances in neural information processing systems*, 2014, pp. 3104–3112.
- [18] F. Yu and V. Koltun, "Multi-scale context aggregation by dilated convolutions," in *4th International Conference on Learning Representations, ICLR 2016, San Juan, Puerto Rico, May 2-4, 2016, Conference Track Proceedings*, 2016.
- [19] Z. Pan, Y. Liang, W. Wang, Y. Yu, Y. Zheng, and J. Zhang, "Urban traffic prediction from spatio-temporal data using deep meta learning," in *Proceedings of the 25th ACM SIGKDD International Conference on Knowledge Discovery & Data Mining, KDD 2019, Anchorage, AK, USA, August 4-8, 2019*. ACM, 2019, pp. 1720–1730.
- [20] L. Bai, L. Yao, C. Li, X. Wang, and C. Wang, "Adaptive graph convolutional recurrent network for traffic forecasting," in *Advances in Neural Information Processing Systems 33: Annual Conference on Neural Information Processing Systems 2020, NeurIPS 2020, December 6-12, 2020, virtual*, 2020.
- [21] C. Shang, J. Chen, and J. Bi, "Discrete graph structure learning for forecasting multiple time series," in *9th International Conference on Learning Representations, ICLR 2021, Virtual Event, Austria, May 3-7, 2021*. OpenReview.net, 2021.
- [22] B. Yu, H. Yin, and Z. Zhu, "Spatio-temporal graph convolutional networks: A deep learning framework for traffic forecasting," in *Proceedings of the Twenty-Seventh International Joint Conference on Artificial Intelligence, IJCAI 2018, July 13-19, 2018, Stockholm, Sweden*, J. Lang, Ed. ijcai.org, 2018, pp. 3634–3640.
- [23] F. Li, J. Feng, H. Yan, G. Jin, F. Yang, F. Sun, D. Jin, and Y. Li, "Dynamic graph convolutional recurrent network for traffic prediction: Benchmark and solution," *ACM Transactions on Knowledge Discovery from Data (TKDD)*, 2021.
- [24] Z. Wu, S. Pan, G. Long, J. Jiang, X. Chang, and C. Zhang, "Connecting the dots: Multivariate time series forecasting with graph neural networks," in *KDD '20: The 26th ACM SIGKDD Conference on Knowledge Discovery and Data Mining, Virtual Event, CA, USA, August 23-27, 2020*. ACM, 2020, pp. 753–763.
- [25] D. Cao, Y. Wang, J. Duan, C. Zhang, X. Zhu, C. Huang, Y. Tong, B. Xu, J. Bai, J. Tong, and Q. Zhang, "Spectral temporal graph neural network for multivariate time-series forecasting," in *Advances in Neural Information Processing Systems 33: Annual Conference on Neural Information Processing Systems 2020, NeurIPS 2020, December 6-12, 2020, virtual*, 2020.
- [26] L. Han, B. Du, L. Sun, Y. Fu, Y. Lv, and H. Xiong, "Dynamic and multi-faceted spatio-temporal deep learning for traffic speed forecasting," in *KDD '21: The 27th ACM SIGKDD Conference on Knowledge Discovery and Data Mining, Virtual Event, Singapore, August 14-18, 2021*. ACM, 2021, pp. 547–555.
- [27] C. Zheng, X. Fan, C. Wang, and J. Qi, "GMAN: A graph multi-attention network for traffic prediction," in *The Thirty-Fourth AAAI Conference on Artificial Intelligence, AAAI 2020, The Thirty-Second Innovative Applications of Artificial Intelligence Conference, IAAI 2020, The Tenth AAAI Symposium on Educational Advances in Artificial Intelligence, EAAI 2020, New York, NY, USA, February 7-12, 2020*. AAAI Press, 2020, pp. 1234–1241.
- [28] X. Wang, Y. Ma, Y. Wang, W. Jin, X. Wang, J. Tang, C. Jia, and J. Yu, "Traffic flow prediction via spatial temporal graph neural network," in *WWW '20: The Web Conference 2020, Taipei, Taiwan, April 20-24, 2020*. ACM / IW3C2, 2020, pp. 1082–1092.
- [29] S. Guo, Y. Lin, H. Wan, X. Li, and G. Cong, "Learning dynamics and heterogeneity of spatial-temporal graph data for traffic forecasting," *IEEE Trans. Knowl. Data Eng.*, vol. 34, no. 11, pp. 5415–5428, 2022.
- [30] S. Guo, Y. Lin, N. Feng, C. Song, and H. Wan, "Attention based spatial-temporal graph convolutional networks for traffic flow forecasting," in *AAAI*, 2019.
- [31] C. Park, C. Lee, H. Bahng, Y. Tae, S. Jin, K. Kim, S. Ko, and J. Choo, "ST-GRAT: A novel spatio-temporal graph attention networks for accurately forecasting dynamically changing road speed," in *CIKM '20: The 29th ACM International Conference on Information and Knowledge Management, Virtual Event, Ireland, October 19-23, 2020*. ACM, 2020, pp. 1215–1224.
- [32] H. Wu, J. Xu, J. Wang, and M. Long, "Autoformer: Decomposition transformers with auto-correlation for long-term series forecasting," in *Advances in Neural Information Processing Systems 34: Annual Conference on Neural Information Processing Systems 2021, NeurIPS 2021, December 6-14, 2021, virtual*, 2021, pp. 22419–22430.
- [33] T. Zhou, Z. Ma, Q. Wen, X. Wang, L. Sun, and R. Jin, "Fedformer: Frequency enhanced decomposed transformer for long-term series forecasting," in *International Conference on Machine Learning, ICML 2022, 17-23 July 2022, Baltimore, Maryland, USA*, ser. Proceedings of Machine Learning Research, vol. 162. PMLR, 2022, pp. 27268–27286.
- [34] S. Liu, H. Yu, C. Liao, J. Li, W. Lin, A. X. Liu, and S. Dustdar, "Pyraformer: Low-complexity pyramidal attention for long-range time series modeling and forecasting," in *The Tenth International Conference on Learning Representations, ICLR 2022, Virtual Event, April 25-29, 2022*. OpenReview.net, 2022.
- [35] A. Zeng, M. Chen, L. Zhang, and Q. Xu, "Are transformers effective for time series forecasting?" 2023.
- [36] S. Li, X. Jin, Y. Xuan, X. Zhou, W. Chen, Y. Wang, and X. Yan, "Enhancing the locality and breaking the memory bottleneck of transformer on time series forecasting," in *Advances in Neural Information Processing Systems 32: Annual Conference on Neural Information Processing Systems 2019, NeurIPS 2019, December 8-14, 2019, Vancouver, BC, Canada*, 2019, pp. 5244–5254.
- [37] N. Kitaev, L. Kaiser, and A. Levskaya, "Reformer: The efficient transformer," in *8th International Conference on Learning Representations, ICLR 2020, Addis Ababa, Ethiopia, April 26-30, 2020*. OpenReview.net, 2020.
- [38] H. Cao, Y. Wang, J. Chen, D. Jiang, X. Zhang, Q. Tian, and M. Wang, "Swin-UNET: UNet-like pure transformer for medical image segmentation," *arXiv preprint arXiv:2105.05537*, 2021.
- [39] A. Dosovitskiy, L. Beyer, A. Kolesnikov, D. Weissenborn, X. Zhai, T. Unterthiner, M. Dehghani, M. Minderer, G. Heigold, S. Gelly, J. Uszkoreit, and N. Houlsby, "An image is worth 16x16 words: Transformers for image recognition at scale," in *9th International Conference on Learning Representations, ICLR 2021, Virtual Event, Austria, May 3-7, 2021*. OpenReview.net, 2021.
- [40] Z. Shao, Z. Zhang, F. Wang, W. Wei, and Y. Xu, "Spatial-temporal identity: A simple yet effective baseline for multivariate time series forecasting," in *Proceedings of the 31st ACM International Conference on Information & Knowledge Management, Atlanta, GA, USA, October 17-21, 2022*. ACM, 2022, pp. 4454–4458.
- [41] J. Deng, X. Chen, R. Jiang, X. Song, and I. W. Tsang, "St-norm: Spatial and temporal normalization for multi-variate time series forecasting," in *KDD '21: The 27th ACM SIGKDD Conference on Knowledge Discovery and Data Mining, Virtual Event, Singapore, August 14-18, 2021*. ACM, 2021, pp. 269–278.
- [42] Z. Liu, Y. Lin, Y. Cao, H. Hu, Y. Wei, Z. Zhang, S. Lin, and B. Guo, "Swin transformer: Hierarchical vision transformer using shifted windows," in *2021 IEEE/CVF International Conference on Computer Vision, ICCV 2021, Montreal, QC, Canada, October 10-17, 2021*. IEEE, 2021, pp. 9992–10002.
- [43] H. V. Jagadish, J. Gehrke, A. Labrinidis, Y. Papakonstantinou, J. M. Patel, R. Ramakrishnan, and C. Shahabi, "Big data and its technical challenges," *Communications of the ACM*, 2014.
- [44] C. Chen, K. Petty, A. Skabardonis, P. Varaiya, and Z. Jia, "Freeway performance measurement system: mining loop detector data," *Transportation Research Record*, 2001.
- [45] Y. Cui, J. Xie, and K. Zheng, "Historical inertia: A neglected but powerful baseline for long sequence time-series forecasting," in *CIKM '21: The 30th ACM International Conference on Information and Knowledge Management, Virtual Event, Queensland, Australia, November 1 - 5, 2021*. ACM, 2021, pp. 2965–2969.
- [46] Y. Zhang and J. Yan, "Crossformer: Transformer utilizing cross-dimension dependency for multivariate time series forecasting," in *The Eleventh International Conference on Learning Representations, ICLR 2023, Kigali, Rwanda, May 1-5, 2023*. OpenReview.net, 2023.
- [47] R. Cirstea, C. Guo, B. Yang, T. Kieu, X. Dong, and S. Pan, "Tri-former: Triangular, variable-specific attentions for long sequence multivariate time series forecasting," in *Proceedings of the Thirty-First International Joint Conference on Artificial Intelligence, IJCAI 2022, Vienna, Austria, 23-29 July 2022*. ijcai.org, 2022, pp. 1994–2001.



Zezhi Shao received the B.E. degree from Shandong University, Jinan, China, in 2019. He is currently pursuing a Ph.D. degree with the Institute of Computing Technology, Chinese Academy of Sciences, China. His research interests include traffic forecasting, multivariate time series forecasting, graph neural networks, and spatial-temporal data mining. He has published several papers in top journals and conferences, such as TKDE, SIGKDD, VLDB, CIKM, etc.



Yongjun Xu is a professor at Institute of Computing Technology, Chinese Academy of Sciences (ICT-CAS) in Beijing, China. He received his B.Eng. and Ph.D. degree in computer communication from Xi'an Institute of Posts & Telecoms (China) in 2001 and Institute of Computing Technology, Chinese Academy of Sciences, Beijing, China in 2006, respectively. His current research interests include artificial intelligence systems, and big data processing.



Fei Wang, born in 1988, PhD, associate professor. He received the B.S. degree in computer science from the Beijing Institute of Technology, Beijing, China, in 2011. He received the PhD degree in computer architecture from Institute of Computing Technology, Chinese Academy of Sciences in 2017. From 2017 to 2020, he was a research assistant with the Institute of Technology, Chinese Academy of Sciences. Since 2020, he has been working as associate professor in Institute of Computing Technology, Chinese

Academy of Sciences. His main research interest includes spatiotemporal data mining, Information fusion, graph neural networks.



Zhao Zhang is an assistant professor at the Institute of Computing Technology, Chinese Academy of Sciences, Beijing, China. He received the B.E. degree in Computer Science and Technology from the Beijing Institute of Technology (BIT) in 2015, and Ph.D. degree in the Institute of Computing Technology, Chinese Academy of Sciences in 2021. His current research interests include data mining and knowledge graphs. He has published more than 20 papers in the prestigious refereed conferences

and journals, such as KDD, SIGIR, WWW and IEEE TKDE.



Yuchen Fang is currently pursuing a Ph.D. at the University of Electronic Science and Technology of China. His general research interests are in spatio-temporal data mining, graph neural networks, and urban computing, with a special focus on traffic forecasting. He has published several papers in top journals and conference proceedings, such as ICDE, SIGIR, AAAI, and TITS.



Guangyin Jin received a B.E. degree from the Department of Mechanical and Electrical Engineering of Xiamen University. Now he is a Ph.D candidate at College of Systems Engineering of National University of Defense Technology. His research interest falls in the area of spatial-temporal data mining, graph neural networks and urban computing. So far, he has published more than ten papers in JCR Q1-level international journals such as TITS, TIST, TRC, INS, and top international conferences such as AAAI,

CIKM, SIGSPATIL. He also serves as the PC member or reviewer for top international conferences or journals such as AAAI, WWW, ECML-PKDD, TITS, TKDD, TRC, etc.